Dielectric response of the degenerate plasma of charged bosons in static-local-field approximations

1994 J. Phys.: Condens. Matter 6 8795

(http://iopscience.iop.org/0953-8984/6/42/011)

J. Phys.: Condens. Matter 6 (1994) 8795–8807. Printed in the UK

Dielectric response of the degenerate plasma of charged bosons in static-local-field approximations

S Conti, M L Chiofalo and M P Tosi
Scuola Normale Superiore, Piazza dei Cavalieri 7, I-56126 Pisa, Italy

Received 12 July 1994

Abstract. The dielectric screening function $\varepsilon(k, \omega)$ of the fluid of charged bosons at zero temperature is evaluated in a range of low-to-intermediate coupling strength, in view of recent data on static screening and fluid structure from quantum Monte Carlo methods. Correlations beyond the random phase approximation are included within a class of approximations which are well known for the electron fluid, i.e. by introducing a frequency-independent local field factor to be determined through self-consistency requirements connecting various aspects of the physics contained in the dielectric function. The static dielectric function $\varepsilon(k, 0)$ is negative over a range of wavenumbers at all values of the density, leading to oscillatory screening of a foreign charge and to an effective long-range attraction between equi-charged impurities. Quantitative agreement with the Monte Carlo data on static screening is achieved by imposing self-consistency on the compressibility of the fluid in addition to self-consistency on the pair distribution function. Good agreement is also obtained on the pair distribution function and the correlation energy. Within the present class of approximations, the dispersion relation of longitudinal excitations takes the Feynman form, starting at the plasma frequency with a negative dispersion coefficient and going through a minimum before ending at the single-particle recoil frequency.

1. Introduction

The fluid of point-like spinless charged bosons embedded in a uniform neutralizing background has drawn some attention in the literature as a model in quantum statistical mechanics with possible applications to superconductors and to systems of astrophysical interest. Quantum Monte Carlo studies of the boson ground state [1, 2] have revealed a scenario paralleling that of the fermion ground state as a function of the dimensionless length parameter $r_s = r_0/a_0$, where r_0 is related to the particle number density n by $r_0 = (4\pi n/3)^{-1/3}$ and a_0 is the Bohr radius. Starting from the ideal Bose gas at $r_s = 0$, correlations in the fluid state grow with increasing r_s till Wigner crystallization occurs at $r_s \approx 160$. More recently, the static dielectric function $\varepsilon(k, 0)$ has been directly determined by quantum Monte Carlo methods [3] from the response of the system to an imposed static sinusoidal electric potential at various values of the wavenumber k and at values of r_s in the fluid and in the crystalline phase. The results have been compared to the random phase approximation (RPA) for the weakly coupled fluid and to classical lattice values for the low-density crystal. Data on the pair distribution function $g(r)$ over a wide range of r_s are also available [3, 4].

On the theoretical side, early evaluations of the ground state energy and the spectrum of elementary excitations in the high-density limit [5, 6], were followed by variational calculations of the ground state over a wide range of r_s using Jastrow wavefunctions [7–9, 1]. Hore and Frankel [10] have given a full analytic evaluation of the dynamic dielectric

0953-8984/94/428795+13$19.50

function $\varepsilon(k, \omega)$ of the fluid at arbitrary temperature within the RPA. This approximation appears to be particularly restrictive for the fluid of interacting bosons at zero temperature, where the ideal boson gas is fully condensed in the zero-momentum state. The role of correlations beyond the RPA has been explored by Caparica and Hipolito [11] and by Gold [12] within the so-called STLS approximation as proposed earlier [13] for the electron fluid. However, a systematic study of alternative theoretical approaches to correlations in the dielectric response of the charged boson fluid is as yet lacking and is indeed timely in view of the recent evidence from simulation studies.

It is the purpose of the present work to present such a study. We comparatively examine the results of alternative schemes treating correlations, as in earlier work on the electron fluid [13–15], through a local field factor taken as a frequency-independent function $G(k)$ to be determined with the help of self-consistency requirements. The physical properties of main interest are the static dielectric function, with special attention to its long-wavelength limit where the question arises of consistency with the equation of state, and the radial distribution function and correlation energy. In addition we use our results on dynamic screening to evaluate the dispersion relation for longitudinal excitations in the fluid. As one may expect, there are striking differences in physical behaviour between the charged boson fluid and the charged fermion fluid in the regime of low-to-moderate coupling strength, but similarities emerge as the density decreases into the strong coupling region [16].

2. Dielectric response

The reciprocal of the dielectric function is defined from the response of the fluid to a weak external potential $V_e(\boldsymbol{r}, t)$ due to a distribution of charges varying in space and time with a wavevector $\boldsymbol{k}$ and a frequency ω [17]. Time-dependent density functional theory [18] ensures that within the linear response regime, the Fourier transform $n(\boldsymbol{k}, \omega)$ of the induced density change $\delta n(\boldsymbol{r}, t)$ can be related to the sum of the Hartree potential and of the short-range correlation potential through the susceptibility $\chi_0(k, \omega)$ of the ideal gas

$$n(\boldsymbol{k}, \omega) = \chi_0(k, \omega)\{V_e(\boldsymbol{k}, \omega) + (4\pi e^2/k^2)[1 - G(k, \omega)]n(\boldsymbol{k}, \omega)\}. \tag{2.1}$$

Here, the short-range correlation potential has been expressed through a dynamic local field factor $G(k, \omega)$ defined by

$$-\frac{4\pi e^2}{k^2}G(k, \omega) = \int \mathrm{d}(\boldsymbol{r} - \boldsymbol{r}') \int \mathrm{d}(t - t')\, f_c(|\boldsymbol{r} - \boldsymbol{r}'|, t - t') \exp[\mathrm{i}\boldsymbol{k} \cdot (\boldsymbol{r} - \boldsymbol{r}') - \mathrm{i}\omega(t - t')] \tag{2.2}$$

where

$$f_c(|\boldsymbol{r} - \boldsymbol{r}'|, t - t') = \frac{\delta^2 A_c[n(\boldsymbol{r}, t)]}{\delta n(\boldsymbol{r}, t)\delta n(\boldsymbol{r}', t')}|_{n(\boldsymbol{r},t)=n}. \tag{2.3}$$

$A_c[n(\boldsymbol{r}, t)]$ is the correlation part of the action integral as a functional of the perturbed density, its second functional derivative being taken in (2.3) at the initial unperturbed density n. Equation (2.1) leads to

$$\varepsilon(k, \omega) = 1 - \frac{(4\pi e^2/k^2)\chi_0(k, \omega)}{1 + (4\pi e^2/k^2)G(k, \omega)\chi_0(k, \omega)}. \tag{2.4}$$

The susceptibility of the ideal Bose gas at zero temperature has the simple expression [10]

$$\chi_0(k,\omega) = (nk^2/m)[\omega(\omega+\mathrm{i}\eta) - (\hbar k^2/2m)^2]^{-1} \tag{2.5}$$

with η a positive infinitesimal.

The van Hove dynamic structure factor $S(k,\omega)$ giving the excitation spectrum of the fluid is related to the dielectric function by

$$S(k,\omega) = -\frac{\hbar k^2}{2\pi n e^2}\theta(\omega)\,\mathrm{Im}\,\frac{1}{\varepsilon(k,\omega)} \tag{2.6}$$

$\theta(\omega)$ being the Heaviside step function. The static structure factor $S(k)$ follows by integration over energy transfer

$$S(k) = \int_{-\infty}^{\infty}\frac{\mathrm{d}\omega}{2\pi}S(k,\omega) \tag{2.7}$$

and hence the radial distribution function $g(r)$ is obtained by Fourier transform

$$g(r) = 1 + \frac{1}{N}\sum_{k}[S(k)-1]\exp(\mathrm{i}\boldsymbol{k}\cdot\boldsymbol{r}). \tag{2.8}$$

The latter function, being by definition the probability that two particles be found at a relative distance r at any given time, allows an evaluation of the mean potential energy E_{pot} per particle

$$E_{\mathrm{pot}} = \frac{1}{2}n\int\mathrm{d}\boldsymbol{r}\,\frac{e^2}{r}[g(r)-1] = \frac{1}{N}\sum_{k}\frac{2\pi n e^2}{k^2}[S(k)-1]. \tag{2.9}$$

Finally, the ground state energy E_{gs} is obtained by integration of E_{pot} over the coupling strength. The virial theorem ensures that the coupling strength is measured by r_s.

A number of sum rules and exact limiting behaviours are known for $\varepsilon(k,\omega)$ and $G(k,\omega)$ in the electron fluid [19–21] and are immediately translated to the boson plasma. Here we note for later reference the following exact relations:

(i) the *compressibility sum rule*, which may be expressed as

$$G(k,0) = \gamma k^2 \qquad (kr_0 \ll 1) \tag{2.10}$$

with

$$\gamma = (4\pi n^2 e^2)^{-1}\left[\frac{1}{K_0} - \frac{1}{K}\right] \tag{2.11}$$

where K and K_0 are the compressibility of the real fluid and of the ideal gas. Since $K_0^{-1} = 0$ for the Bose gas, the role of correlations in adding to the Coulomb repulsion an effective *attractive* interaction between the particles is equivalent to the inequality $K < 0$ at all $r_s > 0$ for bosons.

(ii) the first and third *spectral moment sum rules*

$$M_1(k) = -\frac{k^2}{4\pi^2 e^2}\int_{-\infty}^{\infty}\omega\,\mathrm{Im}\,\frac{1}{\varepsilon(k,\omega)}\,\mathrm{d}\omega = \frac{nk^2}{m} \tag{2.12}$$

and

$$M_3(k) = -\frac{k^2}{4\pi^2 e^2}\int_{-\infty}^{\infty} \omega^3 \,\mathrm{Im}\, \frac{1}{\varepsilon(k,\omega)}\,\mathrm{d}\omega$$
$$= \frac{nk^2}{m}\left\{\omega_{\mathrm{p}}^2 + \frac{2k^2}{m}E_{\mathrm{kin}} + \left(\frac{\hbar k^2}{2m}\right)^2 + \frac{\omega_{\mathrm{p}}^2}{N}\sum_{q(\neq k)} (\hat{q}\cdot\hat{k})^2[S(|k-q|) - S(q)]\right\} \tag{2.13}$$

where $\omega_{\mathrm{p}} = (4\pi ne^2/m)^{1/2}$ and E_{kin} is the mean kinetic energy per particle.

(iii) the *Kimball–Niklasson relations*

$$\frac{\mathrm{d}\ln g(r)}{\mathrm{d}r}|_{r=0} = a_0^{-1} \tag{2.14}$$

and

$$\lim_{k\to\infty} S(k) = 1 - \frac{6r_{\mathrm{s}}}{r_0^4 k^4} g(0). \tag{2.15}$$

Equation (2.15) implies a self-consistency requirement between the asymptotic behaviour of the structure factor and the value of $g(0)$ obtained from (2.8).

3. Static-local-field approximations

The RPA is obtained from (2.4) by setting $G(k,\omega) = 0$. The class of approximations that we examine in the following sections instead neglects the frequency dependence of the local field factor. From (2.4) and (2.5) we then have the excitation spectrum as

$$\mathrm{Im}\,\frac{1}{\varepsilon(k,\omega)} = -\pi\omega_{\mathrm{p}}^2 \mathrm{sign}(\omega)\delta(\omega^2 - \omega_k^2) \tag{3.1}$$

where

$$\omega_k = \{\omega_{\mathrm{p}}^2[1 - G(k)] + (\hbar k^2/2m)^2\}^{1/2}. \tag{3.2}$$

Equations (2.6) and (2.7) yield

$$S(k) = \hbar k^2/2m\omega_k \tag{3.3}$$

which is the Feynman relation. Thus, self-consistency between dielectric response and liquid structure leads for the boson plasma to the relation between $S(k)$ and $G(k)$ given in (3.2) and (3.3).

The approximate closures that we evaluate below involve a further explicit expression of the local field factor in terms of the static structure factor. We consider, first of all, the STLS approximation [13] in which this expression is

$$G_{\mathrm{STLS}}(k) = -\frac{1}{(2\pi)^3 n}\int \frac{k\cdot q}{q^2}[S(|k-q|) - 1]\,\mathrm{d}q. \tag{3.4}$$

As mentioned in section 1, this approximation has already been explored for the boson plasma by Caparica and Hipolito [11] and by Gold [12]. We consider next the approximation proposed by Vashishta and Singwi [14]

$$G_{\mathrm{VS}}(k) = \left(1 + an\frac{\partial}{\partial n}\right) G_{\mathrm{STLS}}(k) \tag{3.5}$$

where a is a parameter which allows one to add self-consistency on the compressibility through (2.10) and (2.11), with K evaluated from the ground-state energy. Finally, we also illustrate the results obtained in the Pathak–Vashishta approximation [15]

$$G_{\mathrm{PV}}(k) = \frac{1}{(2\pi)^3 n} \int \frac{(k \cdot q)^2}{k^2 q^2} [S(|k - q|) - S(q)]\, \mathrm{d}q \tag{3.6}$$

which satisfies the sum rule (2.13) with the exact mean kinetic energy being replaced by its ideal-gas value ($E_{\mathrm{kin}} = 0$ for the ideal Bose gas). We note that all these approximations miss the k^2 term discussed by Holas [21] in the large-k behaviour of $G(k, 0)$ and that only the STLS approximation satisfies consistency between the value of $g(0)$ and the coefficient of the k^{-4} term in (2.15).

3.1. Numerical procedure

The numerical results that we present in the following sections have been obtained by achieving self-consistency between structure factor and local field factor through an iterative method. At each value of r_s we start from the RPA value $G(k; r_s) = 0$ and continue iterations till input and output for $G(k; r_s)$ differ by an amount of order 10^{-5}. The rate of convergence is increased by using as input at each step a weighted average of the outputs from the two previous steps.

The additional self-consistency with the compressibility sum rule in the VS scheme poses some delicate numerical problems in the evaluation of the derivative $G(k; r_s)$ with respect to r_s. Slightly different results are obtained when the derivative is evaluated as the incremental ratio from two neighbouring values of r_s, as was done in the original calculation on the electron fluid [14], or by using input from three or more neighbouring values of r_s. These errors affect the results for $g(r)$ at small r as well as those for $G(k)$ at large k and become increasingly relevant with increasing r_s above $r_s \approx 5$. For this reason the detailed results that we report in the following sections for the VS scheme do not extend beyond $r_s = 30$. They are based on the original two-point-incremental-ratio procedure and our numerical difficulties will be evident in spurious oscillations in $g(r)$ at small r. Such oscillations may be smoothed away by allowing the self-consistency parameter a to become a function of k with a smooth cut-off at large k, thus also recovering self-consistency with the Kimball-Niklasson relation (2.15). However, the location of the cut-off is arbitrary and, of course, the numerical results depend on it.

4. Local field factor, fluid structure and correlation energy

Figure 1 reports our results for the local field factor $G(k)$ in the STLS and VS approximations over a range of r_s from 1 to 30. A peak at $kr_0 \approx 4$ develops in $G(k)$ with increasing r_s and is especially marked in the VS result. According to (2.1), the effective interaction arising from correlations between pairs of particles overbalances their direct Coulomb repulsion in the range of wavenumber where $G(k)$ is above unity, leading here to a net effective attraction between the particles. The emergence of the peak in $G(k)$ is a precursor of Wigner crystallization, the first star of reciprocal lattice vectors of the BCC lattice being in approximate correspondence with the position of the peak. Reference should be made to the work of Senatore and Pastore [22] in relation to Wigner crystallization of the degenerate electron fluid. The corresponding results for the static structure factor $S(k)$ are shown in figure 2, the growing main peak in this function being clearly related to the peak in $G(k)$.

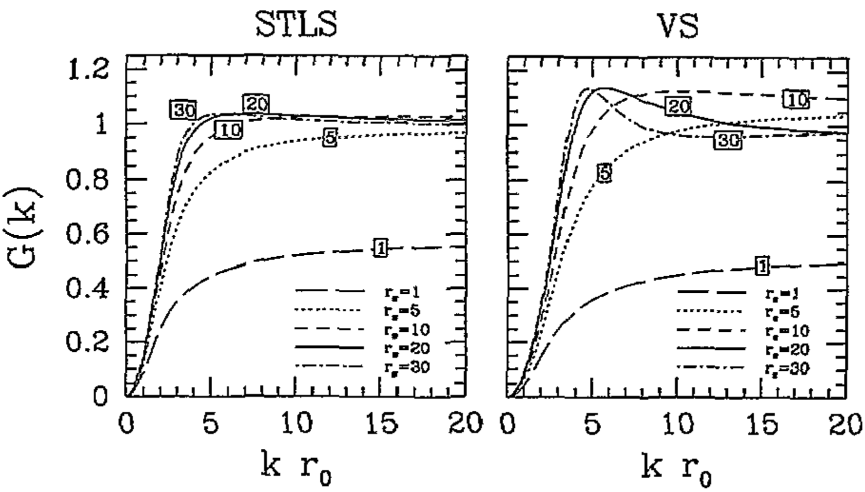

Figure 1. Local field factor $G(k)$ versus kr_0 at various values of r_s in STLS and VS.

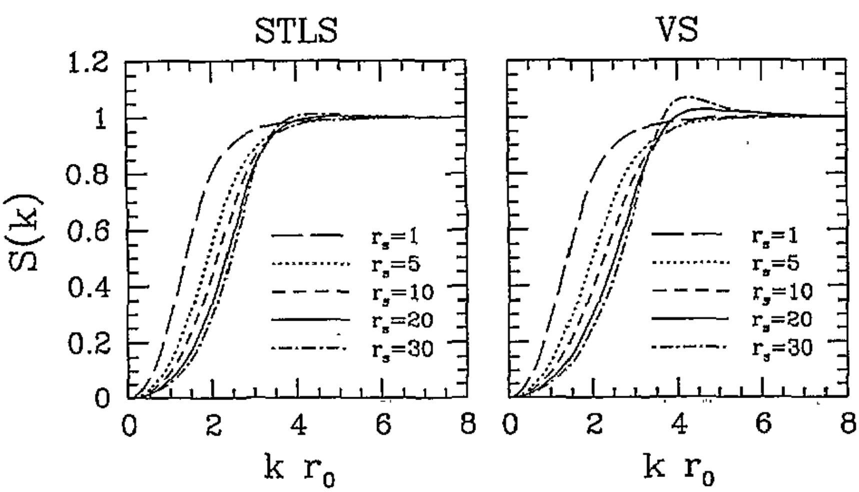

Figure 2. Structure factor $S(k)$ versus kr_0 at various values of r_s in STLS and VS.

The parameter a obtained from self-consistency on the compressibility in the VS scheme shows weak dependence on r_s, our numerical results being accurately reproduced by the fit

$$a(r_s) = 0.833 - 0.007\,47 r_s + 6.63 \times 10^{-5} r_s^2 \qquad (0 < r_s \leqslant 30). \qquad (4.1)$$

These values are similar to those obtained for the electron fluid [14] and again exceed the value $a = 1/2$ that would apply to classical plasma treated in the same approximation. From this element of self-consistency we expect the VS results for $G(k)$ to be quite reliable in the low-k region (see section 5 below).

In fact, the VS scheme also yields satisfactory results for the pair distribution function, excepting the small-r region as discussed already in section 3.1. This is shown in figures 3 and 4, which report $g(r)$ at various values of r_s in comparison with quantum Monte Carlo data from Sugiyama *et al* [13] and from unpublished calculations by Moroni. It is especially rewarding that the VS scheme reproduces the emergence of a first-neighbour shell from Coulomb repulsions with increasing coupling strength. The STLS results are somewhat more accurate only at low r_s (see in particular the case $r_s = 1$ in figure 3), while the structural predictions of the PV approach are quite poor at all r_s. We infer from this comparison with the simulation data that the peak structures shown by the VS $G(k)$ and $S(k)$ in figures 1 and 2 are quite realistic.

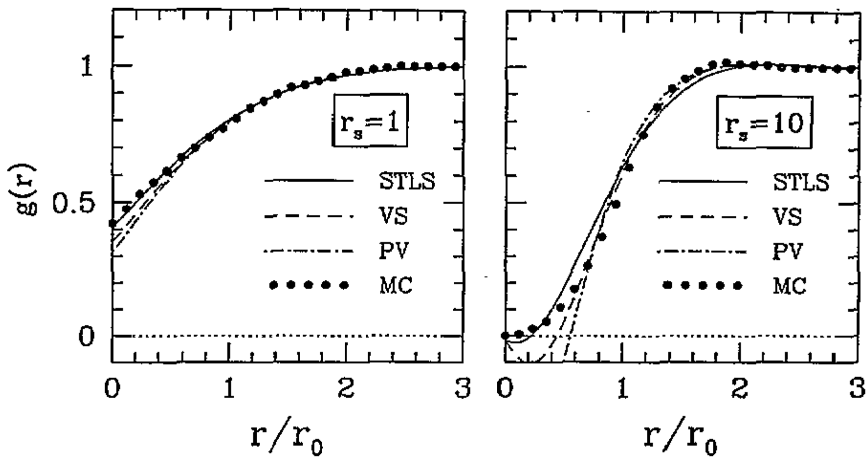

Figure 3. Radial distribution function $g(r)$ versus r/r_0 at $r_s = 1$ and $r_s = 10$ in STLS, VS and PV, compared with quantum Monte Carlo data from [3].

In summary, the quantitative usefulness of the approximations that we have examined is limited to the range of low-to-intermediate coupling strength, with a clear preference for the VS approach from the structural point of view notwithstanding its numerical inaccuracies in the deep part of the Coulomb hole. The STLS and VS approximations are also reasonably accurate in their predictions on the ground-state energy $E_{gs}(r_s)$ and on the pressure $P(r_s)$. A comparison of our results with those obtained by variational methods and with Monte Carlo data is given in tables 1 and 2. Table 3 reports the self-consistent values of the inverse compressibility in the VS approximation.

5. Static screening

We have already noticed in section 2 that the compressibility of the boson plasma is negative at all $r_s > 0$, the ground-state energy being entirely due to correlations. In fact, the static dielectric function is negative at all $r_s > 0$ over a range of reduced wavenumber kr_0 which

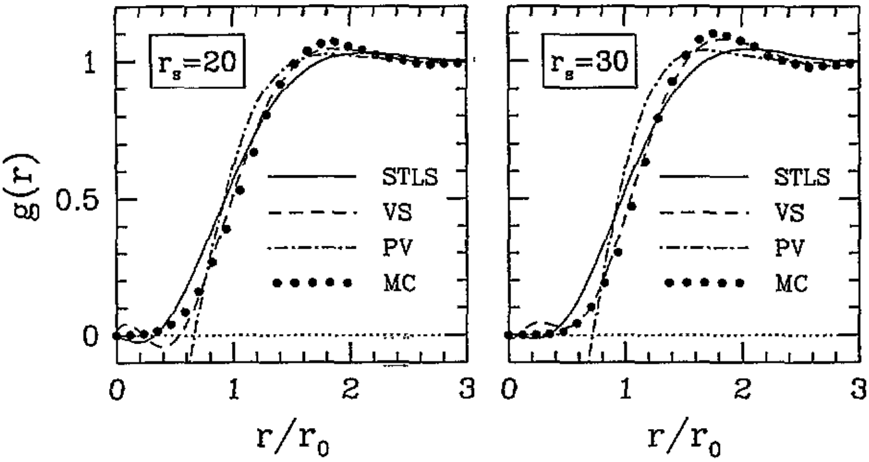

Figure 4. Radial distribution function $g(r)$ versus r/r_0 at $r_s = 20$ and $r_s = 30$ in STLS, VS and PV, compared with quantum Monte Carlo data from S Moroni (unpublished).

Table 1. Values of $-E_{gs}(r_s)$ for the boson plasma (Rydberg/particle).

	Dielectric approach			Monte Carlo		Variational	
r_s	STLS	VS	PV	HM[1]	CA[2]	LR[8]	HM[1]
0.1	4.482	4.496	4.500	—	—	4.489	—
1	0.7712	0.7830	0.7870	—	—	0.7767	0.7810
2	0.4472	0.4578	0.4619	0.453 57	0.4531	0.4516	0.4547
3	0.3232	0.3326	0.3370	—	—	0.3270	0.3288
5	0.2129	0.2207	0.2253	—	0.216 63	0.2159	0.2170
10	0.1188	0.1238	0.1289	—	0.121 50	0.1209	0.1216
20	0.064 86	0.0675	0.0724	0.066 32	0.066 66	0.066 26	0.066 67
30	0.045 07	0.046 74	0.051 12	—	—	0.046 19	0.4644
50	0.028 22	0.029 21	0.032 59	—	0.029 27	—	—
60	0.023 82	—	—	—	—	—	0.024 69
100	0.014 73	—	—	—	0.015 427	0.015 33	0.015 35

Table 2. Values of $-P(r_s)/n$ for the boson plasma (Rydberg/particle).

	Dielectric approach			
r_s	STLS	VS	PV	Variational[1]
0.1	1.129	1.129	1.129	—
1	0.2002	0.2007	0.2007	0.201 05
2	0.1185	0.1193	0.1192	0.119 39
3	0.0870	0.087 99	0.0878	—
5	0.058 68	0.059 85	0.059 67	0.059 115
10	0.033 94	0.035 19	0.035 15	0.034 488
20	0.019 22	0.020 19	0.020 47	0.019 544
30	0.013 62	0.014 37	0.014 80	—
60	0.007 405	—	—	0.007 532
80	0.005 711	—	—	0.005 817
100	0.004 656	—	—	0.004 750

Table 3. Self-consistent values of $-[nK(r_s)]^{-1}$ for the boson plasma in the VS approximation (Rydberg/particle).

r_s	0.1	1	2	3	5	10	20	30
$-[nK(r_s)]^{-1}$	1.41	0.251	0.149	0.110	0.0750	0.0443	0.0258	0.0184

broadens with increasing r_s. This is shown in figure 5, reporting $1/\varepsilon(k,0)$ in the VS approach at values of r_s from 1 to 30. Figure 6 compares our theoretical results for $1/\varepsilon(k,0)$ at $r_s = 1$ and $r_s = 10$ with the quantum Monte Carlo data of Sugiyama *et al* [3]. It is clear that the VS achieves quantitative agreement with the simulation data, within their statistical accuracy and over the restricted range of wavenumber that they cover. Unfortunately, at $r_s = 10$ this range does not extend much beyond the parabolic regime shown in (2.10) and it would be important to extend the simulation to higher values of k for a full test of the theory. It is also evident that the inclusion of short-range correlations through a local field factor is important for bosons even at low coupling. The RPA sets $K^{-1} = 0$ in the dielectric function and hence misses completely the range of negative values for $\varepsilon(k,0)$.

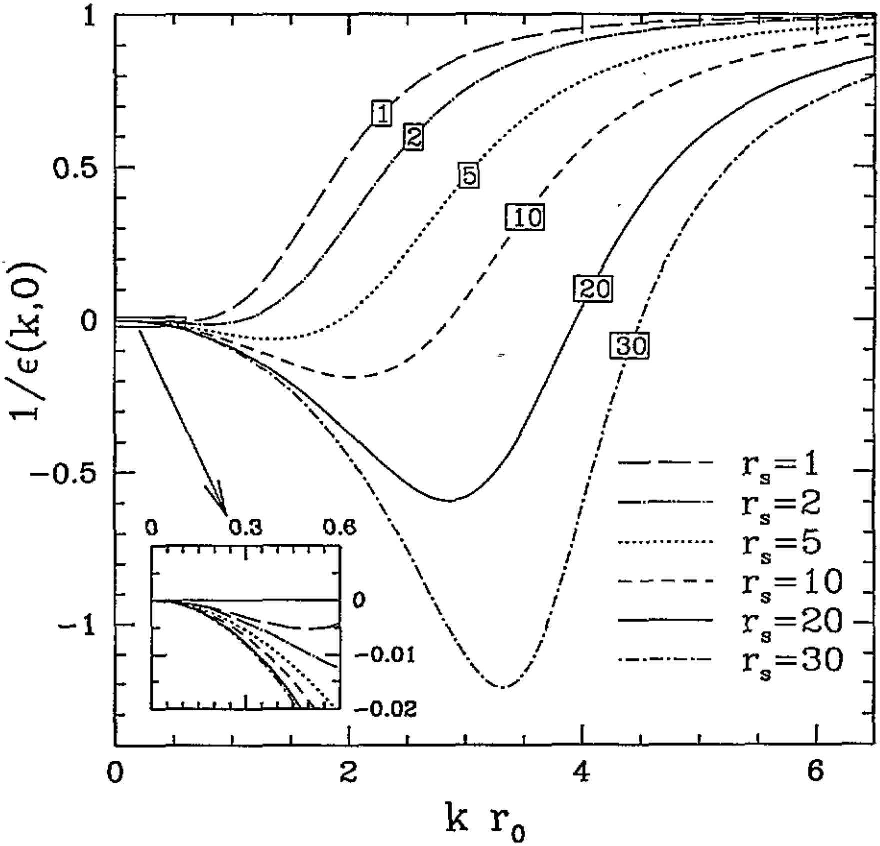

Figure 5. Reciprocal of the static dielectric function $1/\varepsilon(k,0)$ versus kr_0 at various values of r_s in VS. The inset gives an enlarged view of the small-kr_0 region.

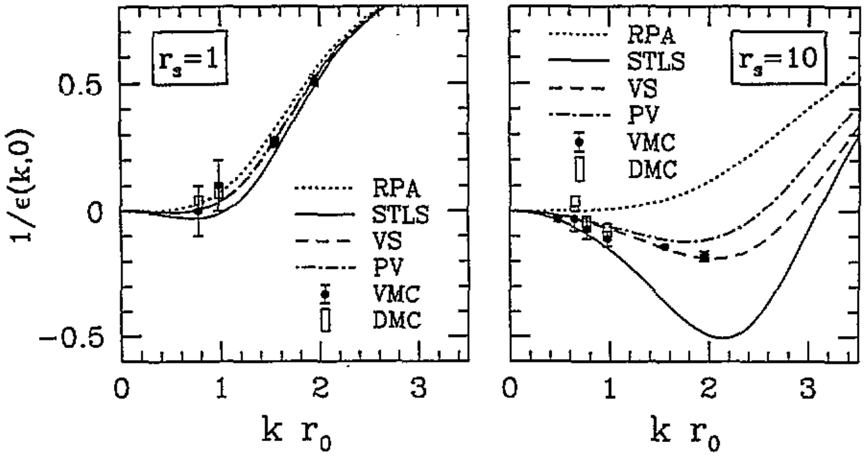

Figure 6. Reciprocal of the static dielectric function $1/\varepsilon(k, 0)$ versus kr_0 at $r_s = 1$ and $r_s = 10$ in RPA, STLS, VS and PV, compared with quantal simulation data from [3] (dots with error bars and rectangles are from variational Monte Carlo and from diffusion Monte Carlo, respectively).

The behaviour of the static dielectric function shown in figures 5 and 6 implies overscreening of a charged impurity. The local pile-up of screening charge in the immediate neighbourhood of the foreign charge exceeds it and hence the displaced charge density oscillates in space, the local enhancements and depletions of charge being overemphasized as a consequence of the statistics. Evidently, the effective interaction between equi-charged impurities in the boson fluid that one would estimate within a linear approximation is attractive over a substantial range of wavenumber, corresponding to distances which tend with increasing r_s to extend down to the mean boson–boson distance.

The asymptotic large-r behaviour of the screening charge density $n_s(r)$ around a point-like impurity carrying unitary charge is [11]

$$n_s(r) \to \frac{b^2}{2\pi r}(1-\gamma^2 b^4)^{-1/2}\sin[br(1+\gamma b^2)^{1/2}]\exp[-br(1-\gamma b^2)^{1/2}] \tag{5.1}$$

where $br_0 = (3r_s)^{1/4}$. Figure 7 illustrates the behaviour of the quantity $4\pi r^2 n_s(r)$ in the VS approximation at various values of r_s. For instance, at $r_s = 10$ we find by integration of $4\pi r^2 n_s(r)$ between its successive nodes that the amounts of screening charge contained in the first four shells around a unitary foreign charge are 1.57, −0.72, 0.18 and −0.04. The inclusion of the factor $r_s^{1/4}$ in the abscissa in figure 7 is suggested by (5.1) and places the nodes of the screening charge distribution in approximate coincidence at different values of r_s.

6. Longitudinal excitations

A static-local-field approximation is clearly a most drastic one in the evaluation of the excitation spectrum. As is shown in (3.1) and (3.2), it yields for the boson plasma a longitudinal excitation with a dispersion curve which goes continuously from the plasma frequency ω_p at $k \to 0$ to the single-particle recoil frequency $\hbar k^2/2m$ at $k \to \infty$. One may recall the well known limitations of the Feynman formula in accounting for the inelastic

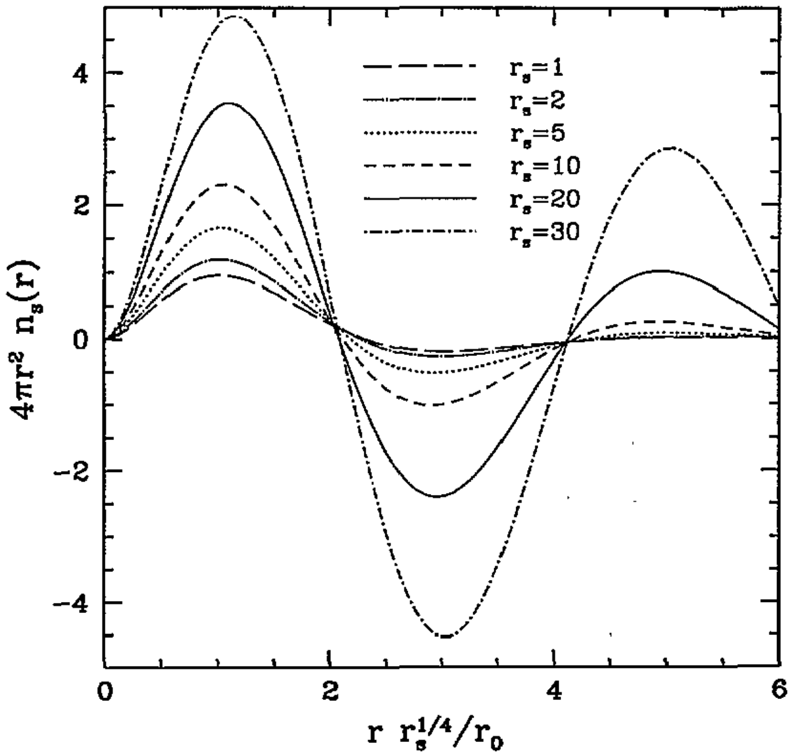

Figure 7. Screening charge density $4\pi r^2 n_s(r)$ around a heavy impurity versus $(r/r_0)r_s^{1/4}$ at various values of r_s in VS.

neutron scattering spectrum from liquid ^{4}He [23]. The observed spectrum contains a branch of collective excitations, including phonons (replaced by plasmons in the boson plasma) and rotons, as well as a broad multi-excitation component. The former branch flattens out and broadens away at about twice the frequency of the roton minimum, while the central frequency of the multi-excitation band increases with k and terminates at the recoil frequency.

Equations (3.2) and (2.10) yield the dispersion of the plasmon at long wavelengths as

$$\omega_k = \omega_p(1 - \tfrac{1}{2}\gamma k^2 + \cdots). \tag{6.1}$$

Thus, within the present class of approximations the dispersion coefficient is directly related to the compressibility of the fluid and is negative at all values of r_s. In a strongly correlated system less energy is needed to excite a vibrational mode in which the particles are partly localized. Notice that in the RPA the leading dispersion term is positive and of order k^4.

Bearing in mind that our results for the full dispersion curve of longitudinal excitations can only have an illustrative value, we report them in figure 8 at various values of r_s in the VS approximation. It is easily seen that $\omega_k \leqslant \omega_p$ over the whole range of wavenumbers where the static dielectric function is negative: indeed, the latter may be written in the form

$$1/\varepsilon(k, 0) = 1 - \omega_p^2/\omega_k^2. \tag{6.2}$$

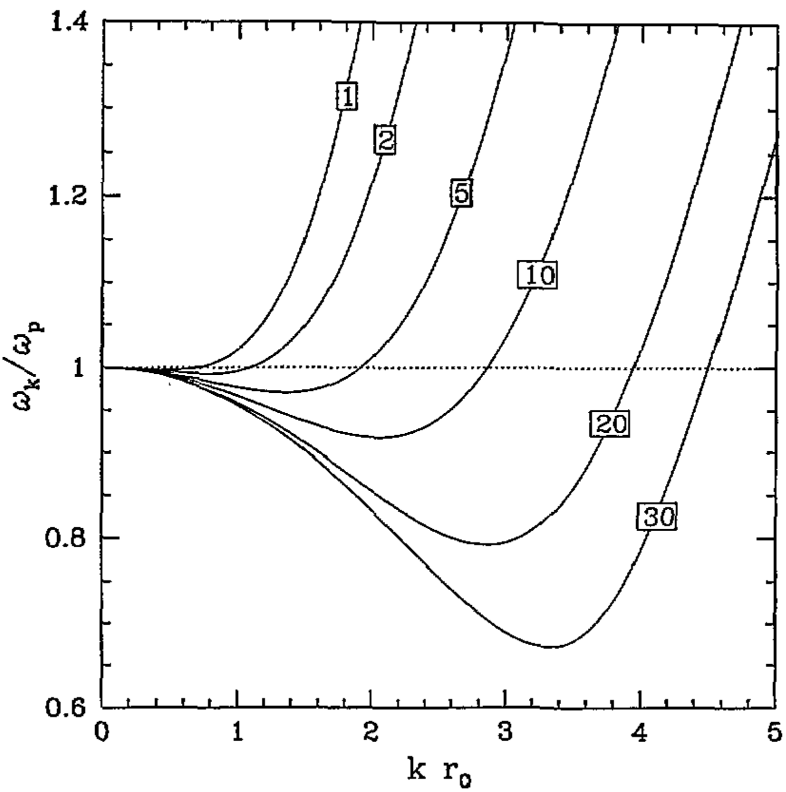

Figure 8. Normalized excitation frequency ω_k/ω_p versus kr_0 at various values of r_s in VS.

Thus, the calculated dispersion curves go through a minimum, whose position and depth in reduced units increase with r_s, before rising rapidly at higher wavenumbers on their approach to the single-particle parabola. Similar but quantitatively different results are obtained in the STLS and PV approximations.

7. Summary and closing remarks

We have seen that short-range correlations play a major role in the static and dynamic dielectric response of the boson plasma at zero temperature and that useful results can be obtained at low-to-moderate values of the coupling strength by means of approximate treatments that were developed quite some time ago for the degenerate electron fluid. With regard to the relative merits of the various expressions that we have considered in relating the local field factor to the structure of the fluid, we have found again that the thermodynamic self-consistency embodied in the VS scheme is crucial for quantitative accuracy in the evaluation of static screening, at least at relatively long wavelengths. It also leads to substantial improvement in the description of how the local structure of the plasma develops with increasing coupling strength.

The dispersion curves for longitudinal excitations that we have reported for the charged boson fluid show some remarkable qualitative features, but also provide an illustration of the limitations of our approach when they are contrasted with the more complex dynamics of liquid ^{4}He. One may learn from them that there is a need to include some account of the frequency dependence of the correlation field factor, together with an explicit account of the correlations in the particle motions that are responsible for the real distribution of momenta. Some progress on these aspects of the theory has recently been made for two-dimensional electron fluids [24] and a parallel theoretical effort on bosons and fermions may be helpful to disentangle the effects due to Coulomb correlations and those due to exchange and the exclusion principle.

Acknowledgments

We are very grateful to Dr S Moroni for making available to us unpublished results on the pair distribution function of the degenerate boson plasma. This work was sponsored by the Ministero dell'Università e della Ricerca Scientifica e Tecnologica of Italy through the Consorzio Interuniversitario Nazionale di Fisica della Materia.

References

[1] Hansen J P and Mazighi R 1978 *Phys. Rev.* A **18** 1282
[2] Ceperley D M and Alder B J 1980 *Phys. Rev. Lett.* **45** 566
[3] Sugiyama G, Bowen C and Alder B J 1992 *Phys. Rev.* B **46** 13 042
[4] Ceperley D M and Alder B J 1980 *J. Physique Coll.* C7 295
[5] Foldy L L 1961 *Phys. Rev.* **124** 649
[6] Brueckner K A 1967 *Phys. Rev.* **156** 204
[7] Lee D K 1970 *Phys. Rev.* A **2** 278
[8] Lee D K and Ree F H 1972 *Phys. Rev.* A **5** 814
[9] Monnier R 1972 *Phys. Rev.* A **6** 393
[10] Hore S R and Frankel N E 1975 *Phys. Rev.* B **12** 2619
[11] Caparica A A and Hipolito O 1982 *Phys. Rev.* A **26** 2832
[12] Gold A 1992 *Z. Phys.* B **89** 1
[13] Singwi K S, Tosi M P, Land R H and Sjölander A 1968 *Phys. Rev.* **176** 589
[14] Vashishta P and Singwi K S 1972 *Phys. Rev.* B **6** 875
[15] Pathak K N and Vashishta P 1973 *Phys. Rev.* B **7** 3649
[16] Chiofalo M L, Conti S and Tosi M P *Mod. Phys. Lett.* B at press
[17] Pines D and Nozières P 1966 *The Theory of Quantum Liquids* vol 1 (New York: Benjamin)
[18] Gross E K U and Kohn W 1990 *Adv. Quant. Chem.* **21** 255
[19] Singwi K S and Tosi M P 1981 *Solid State Phys.* **36** 177
[20] Ichimaru S 1982 *Rev. Mod. Phys.* **54** 1017
[21] Holas A 1986 *Strongly Coupled Plasma Physics* ed F J Rogers and H E DeWitt (New York: Plenum) p 463
[22] Senatore G and Pastore G 1990 *Phys. Rev. Lett.* **64** 303
[23] Woods A D B and Cowley R A 1973 *Rep. Prog. Phys.* **36** 1135
[24] Neilson D, Swierkowski L, Sjölander A and Szymanski J 1991 *Phys. Rev.* B **44** 6291